

Dimensionality dependence of optical nonlinearity and relaxation dynamics in cuprates

M. Ashida,¹ Y. Taguchi,² Y. Tokura,^{2,3} R.T. Clay,^{1,4} S. Mazumdar,⁴ Yu. P. Svirko,¹ and
M. Kuwata-Gonokami^{1,2*}

¹*Cooperative excitation Project, ERATO, Japan Science and
Technology Corporation (JST), Kanagawa 213-0012, Japan*

²*Department of Applied Physics, the University of Tokyo, Tokyo 113-8656, Japan*

³*Correlated Electron Research Center (CERC) and Joint Research Center for Atom Technology
(JRCAT), Tsukuba 305-8562, Japan*

⁴*Department of Physics and the Optical Sciences Center, University of Arizona, Tucson, AZ
85721*

(November 12, 2018)

Abstract

Femtosecond pump-probe measurements find pronounced dimensionality dependence of the optical nonlinearity in cuprates. Although the coherent two-photon absorption (TPA) and linear absorption bands nearly overlap in both quasi-one and two-dimensional (1D and 2D) cuprates, the TPA coefficient is one order of magnitude smaller in 2D than in 1D. Furthermore, picosecond recovery of optical transparency is observed in 1D cuprates, while the recovery in 2D involves relaxation channels with a time scales of tens of picoseconds. The experimental results are interpreted within the two-band extended Hubbard model.

Transport and magnetic behavior of strongly correlated electron (SCE) systems, which depend on the lowest excitations, have been studied extensively in recent years. High energy electronic excitations, in contrast, have received less attention. Linear absorption studies,

performed for the copper oxide based SCE systems [1], do not reveal features associated with optically dark two-photon states. Femtosecond spectroscopic studies in quasi-two dimensional (2D) cuprates [2,3] have revealed the strong role played by magnetic excitations in ultrafast non-radiative relaxation processes, which is related to the large Heisenberg exchanges in the cuprates [4–8]. More recently, interest has shifted to nonlinear optical studies which provide information about both odd parity one-photon states and even parity two-photon states [9–11].

An additional motivation to study nonlinear optical properties of SCE materials originates from the continued quest for new materials with ultrafast and strong optical nonlinearity. The mechanism of optical nonlinearity in SCE systems [12] is different from that in band insulators, and it is conceivable that new SCE materials can be found with nonlinear optical properties that meet the requirements for technological applications. Initial support for this idea has come from the demonstrations of strong two-photon absorption (TPA) along with picosecond recovery of optical transparency in the quasi-one dimensional (1D) cuprate Sr_2CuO_3 [9], and of giant electro-reflectance in several 1D Mott insulators [10]. An important new question that has arisen involves the role of dimensionality in SCE nonlinear optical materials. In conventional band insulators confinement of the Wannier exciton in 1D can strongly enhance the optical nonlinearity [13]. Whether or not similar dimensionality effects occur in SCE systems has not been investigated systematically so far. In the present work we compare the results of the sub-picosecond pump-probe transmission measurements in 1D and 2D cuprates. We observe significant dimensionality dependences in the magnitude of the nonlinear response as well as the relaxation dynamics, which are explained using cluster calculations within the appropriate extended Hubbard Hamiltonian.

To clarify the dimensionality dependence systematically, we selected three materials, which are well-known strongly correlated 1D and 2D charge-transfer (CT) insulators. Specifically, Sr_2CuO_3 (see Fig. 1(a)) and SrCuO_2 (Fig. 1(b)) have single and weakly coupled double Cu-O chains, respectively [6,8]. Since in SrCuO_2 the interchain coupling due to 90° Cu-O-Cu bonds is much weaker than the coupling along the 180° intrachain Cu-O-Cu bonds, this

material can be also classified as a 1D spin system [6,8]. $\text{Sr}_2\text{CuO}_2\text{Cl}_2$ (Fig. 1(c)) is a 2D cuprate with the same CuO_2 network as in La_2CuO_4 with the apical oxygens of the latter replaced with Cl ions [1]. Importantly, the lattice constants in the Cu-O chain direction in these materials are almost same. All of these materials show optical gaps around 2 eV, which corresponds to CT excitation, and are nearly transparent below 1.5 eV (see Fig. 3). The strong antiferromagnetic exchange interaction between holes on neighboring Cu sites, $J \sim 2000 - 3000$ K for Sr_2CuO_3 and SrCuO_2 [6–8] and $J \sim 1400$ K for $\text{Sr}_2\text{CuO}_2\text{Cl}_2$ [4,5], gives rise to wide spinon and magnon bands in 1D and 2D materials, respectively. In spite of the one-dimensionality of Sr_2CuO_3 , a spin-Peierls transition does not occur in this system.

Single crystals of Sr_2CuO_3 and SrCuO_2 are grown by the traveling- solvent floating-zone method [6], while $\text{Sr}_2\text{CuO}_2\text{Cl}_2$ is grown by cooling the stoichiometric melt [4]. Thin flakes with thickness of 50-100 μm are cleaved out for transmission measurements. Two optical parametric generators pumped by a KHz regenerative amplifier generate pump and probe pulses. By using second harmonic and difference frequency generation techniques, the laser system can generate pulses with a temporal width of 0.2 ps and photon energy from 0.3 to 1.5 eV. We measure differential transmission $\Delta T/T$, where T is the transmission in the absence of the pump pulse, as a function of the pump-probe delay. The pump and probe beams are polarized along the Cu-O chains (b axis in Sr_2CuO_3 , c axis in SrCuO_2 and a axis in $\text{Sr}_2\text{CuO}_2\text{Cl}_2$).

The temporal behavior of the photoinduced absorption change at 290 K, $\Delta\alpha L = -\ln(1+\Delta T/T)$, where L is sample thickness, are shown in Fig. 2 for all the three materials with the pump intensity $I_{pump} \sim 0.2$ GW/cm². The 2D material shows absorption change for both co- and cross-polarizations of the pump and probe beams, regardless of the angle between the polarization of the pump light and the crystallographic axes. We have found that $\Delta\alpha L \propto I_{pump}$ up to $I_{pump} \sim 10$ GW/cm² and $I_{pump} \sim 1$ GW/cm² for 1D and 2D materials, respectively. This indicates that the nonlinear effect is third-order in the light field up to these I_{pump} . One can observe from Fig. 2(a) that the temporal profile of $\Delta\alpha L$ in Sr_2CuO_3 consists of a prompt component, which is determined by the laser pulse duration,

and a slowly decaying component with characteristic time ~ 1 ps. From comparisons of the temporal profiles at various pump photon energies we conclude that the relative magnitude of the decay component decreases with decreasing pump photon energy. The temporal profile of $\Delta\alpha L$ in SrCuO₂ (Fig. 2(b)) is similar to that in Sr₂CuO₃. On the other hand, in Sr₂CuO₂Cl₂, there exists a slower component with characteristic time ~ 30 ps as well as the faster component with ~ 1 ps (see the upper panel of Fig. 2).

The prompt component of $\Delta\alpha L$ is due to the coherent optical nonlinearity associated with TPA. In Fig. 3 we have shown the TPA spectra, plotted against $\omega_{pump} + \omega_{probe}$, for all three materials. In all cases, one- and two-photon absorption maxima nearly coincide indicating that overlapping TPA and linear absorption bands is a common feature of cuprates. The TPA spectrum of Sr₂CuO₃ at 290 K is similar to that obtained at 10 K, with maximum $\beta \sim 150$ cm/GW at 2.1 eV [9]. We further observe from Fig. 3 that while in the 1D systems Sr₂CuO₃ and SrCuO₂ β is of the order of 100 cm/GW and the width of the TPA band is about 0.5 eV, in Sr₂CuO₂Cl₂ the TPA coefficient is one order of magnitude smaller and the TPA band is broader. In particular, the low energy tail of the TPA in Sr₂CuO₂Cl₂ continues down to $\omega_{pump} + \omega_{probe} \sim 1.5$ eV, while the TPA coefficient in 1D materials falls below 0.1 cm/GW at 1.5 eV.

In order to understand the differences in the TPA spectra between the 1D and 2D systems, we adopted the two-band extended Hubbard model, which enables us to take into account the CT nature of the excited states explicitly,

$$\begin{aligned}
H = & -t \sum_{\langle ij, \sigma \rangle} (c_{i\sigma}^\dagger c_{j\sigma} + c_{j\sigma} c_{i\sigma}^\dagger) + \sum_i U_i n_{i\uparrow} n_{i\downarrow} \\
& + V \sum_{\langle ij \rangle} n_i n_j + \sum_i \epsilon_i n_i,
\end{aligned} \tag{1}$$

where $c_{i\sigma}^\dagger$ creates a hole with spin σ on site i , $n_{i\sigma} = c_{i\sigma}^\dagger c_{i\sigma}$, $n_i = \sum_\sigma n_{i\sigma}$, and $\langle ij \rangle$ implies nearest-neighbor sites. In Eq. (1), t is the hopping between Cu and O sites, U_i is the on-site Coulomb repulsion between two holes (different on Cu and O sites), V is the Coulomb repulsion between holes on neighboring Cu and O, and $\epsilon_O - \epsilon_{Cu}$ is the site energy difference between O and Cu sites.

It is instructive to first consider the qualitative difference between 1D and 2D within Eq. (1). There exists a single mirror plane in 1D, and optical transitions are between symmetry subspaces that are “plus” and “minus” with respect to this mirror plane. Consider now a three-atom segment OCuO. The single hole in the segment can occupy the Cu-site or either of the two O-sites. We denote these by the “cartoon” configurations 010, and 100 and 001, respectively. The ground state, as well as the excited + symmetry two-photon state are superpositions of 010 and (100 + 001), while the – symmetry optical state is simply (100 – 001). The dipole operator μ within Eq. (1) is $\sum_i \vec{r}_i n_i$ (we take electronic charge $e = 1$), where \vec{r}_i gives the vector location of each atom, and has nonzero matrix element between the configurations (100 + 001) and (100 – 001). The strength of the dipole coupling between the one-photon state and the ground (two-photon) state, μ_{01} (μ_{12}), then depends on the “overlap” between the (100 – 001) one-photon state and the (100 + 001) component of the ground (two-photon) state.

Consider now the 2D case, where each plaquette consists of one Cu and four O-atoms, again with a single hole. There occur two mirror planes now, and the symmetry subspaces are + +, + –, – + and – – with respect to these. Eigenstates in the + + subspace are now superpositions of the configuration with the hole on the Cu, and *four* configurations with the hole occupying the different O-atoms. This subspace contains both the ground state and a two-photon state. The optical states are in the +- and -+ subspaces, are degenerate, and are still superpositions of only *two* configurations each: the +- eigenstate is a superposition of the two configurations with holes on the O-atoms to the left and to the right of the central Cu, while the -+ eigenstate is composed of the configurations with the holes above and below the Cu. The dipole coupling between the one-photon and ++ states then can involve only two of the four configurations with holes on O-sites. Therefore, the transition dipole moments between the ground and one-photon states, μ_{01} , and one- and two-photon states, μ_{12} , are smaller in the 2D than in 1D. Since α and β are proportional to μ_{01}^2 and $\mu_{01}^2 \mu_{12}^2$, respectively [14], we expect both linear absorption and TPA to be weaker in 2D than in 1D, with the reduction in TPA strength larger. The above physical arguments for

small-size cluster picture are valid even with a single electron, indicating that the weaker TPA in 2D can be explained without introducing charge-spin decoupling in 1D, as has been previously claimed [15].

We have verified the above qualitative reasonings by exact diagonalization studies of 1D and 2D clusters containing 4 Cu atoms (see Fig. 4). The 2D cluster chosen is the largest system that can be diagonalized exactly. The choice of the 1D cluster size was based on the requirement that the number of holes are the same in 1D and 2D. The parameters considered were $|t| = 1.4$ eV, $U_{\text{Cu}} = 10$ eV, $U_{\text{O}} = 3$ eV, $V = 1$ eV and $\epsilon_{\text{O}} - \epsilon_{\text{Cu}} = 2$ eV. In Fig. 4, we have shown the lowest energy levels, along with the mirror planes σ in 1D and σ_x and σ_y in 2D. The very low energy excited states in the $+$ subspace in 1D and $++$ subspace in 2D in Fig. 4 are spin excitations that play no direct role in optical nonlinearity and are not discussed further. The calculated electronic structure and the identification of optically relevant states are consistent with the recent group-theoretical analysis based on the excitonic cluster model [11].

Our numerical results can be summarized as follows: (i) The dipole couplings of the ground state with the lowest pair of $+-$ and $-+$ states in 2D are one order of magnitude smaller than that with the next higher pair of $+-$ and $-+$ states in the 2D lattice. Accordingly, the optical states in 2D is a *higher energy* pair of $+-$ and $-+$ states (see Fig. 4). μ_{01}^2 in 2D is 0.36 in our units, as compared to $\mu_{01}^2 \simeq 1$ in the 1D cluster, thereby explaining the weaker linear absorption in 2D (see Fig. 3). (ii) As seen in Fig. 4, in 2D, there exist even parity states, which are antisymmetric with respect to both σ_x and σ_y ($--$ subspace). TPA to these states should occur for cross-polarized pump and probe beams. We have observed the TPA with the cross-polarized configuration in our experiments and will discuss these elsewhere. Note that any interaction (electron-phonon interaction, intrinsic asymmetry due to crystal twinning) that leads to violation of this strict symmetry principle will cause weak TPA to $--$ states even with co-polarized pump and probe. It is conceivable that the broad nature of the TPA in 2D in the high energy region and the persistence of weak TPA in the low energy region (~ 1.5 eV) in $\text{Sr}_2\text{CuO}_2\text{Cl}_2$ (see Fig. 3) are due to the $--$ states. As

seen in Fig. 4, there also exists a $--$ state that occurs below the true optical states. This state was not found in the previous one-band model [15] (presumably because the smaller lattice investigated there did not have the symmetry of the 2D lattice). (iii) In 2D, the most dominant two-photon states are the lowest and the third charge excitation states in the $++$ subspace, whose dipole couplings are 1.25 and 1.35 to the two one-photon states, compared to dipole couplings of 3.4 and 1.2 between the dominant two-photon states and the optical state in 1D. The lower of the two $++$ excited states occurs slightly below the one-photon states in 2D for the parameters we have chosen, but with small modifications of these parameters it can also occur slightly above the one-photon states. Thus in both 1D and 2D the dominant two-photon states are close to the one-photon states in energy, in agreement with experiment. The numerical simulation predicts TPA in 1D larger by roughly one order of magnitude than in 2D even from these small cluster calculations. As discussed above, this is a consequence of the larger coordination number in 2D. (iv) We have included direct O–O hopping up to $|t|/3$ into Hamiltonian (1) and found no changes in our above conclusions.

The other distinct dimensionality dependence is the difference in the relaxation time. Specifically, in $\text{Sr}_2\text{CuO}_2\text{Cl}_2$, there exist decay components with characteristic time ~ 30 ps and ~ 1 ps, while 1D materials show only the latter component. The intensity of the decay components reduces with an decrease in pump photon energy (see Fig. 2). This indicates that the decay mechanism is associated with excitation of real carriers. We ascribe the 1 ps relaxation to non-radiative channels through spinon (in 1D) or magnon (in 2D) states, which exist below the optical gap and whose width is ~ 1 eV [2,9]. We ascribe the slower 30 ps optical relaxation in $\text{Sr}_2\text{CuO}_2\text{Cl}_2$ to the existence of low energy $+ -$ and $- +$ states with weak dipole coupling to the ground state and the forbidden $--$ electronic state that can act as trap states upon photoexcitation (see Fig. 4). Such subgap electronic excitations are absent in 1D, and therefore the trapping of the optical excitation cannot occur. We note that the undoped 2D cuprates $\text{YBa}_2\text{Cu}_3\text{O}_6$ and Nd_2CuO_4 have also shown two decay components with comparable decay rates [2].

In conclusion, pronounced dimensionality dependence of the optical nonlinearity in the cuprates is found experimentally and theoretically. Coherent optical nonlinearity is dominated by two-photon states whose energy locations relative to the optical states are same in both 1D and 2D materials. However, large nonlinearity and ultrafast relaxation are characteristics of only 1D SCE systems, which make them promising materials for ultrafast optoelectronics [9]. The spin excitations with large energies, promoting the relaxation, are unique to SCE systems. The smaller nonlinearity in 2D is due to the larger coordination number of the atoms, and the occurrence of a slower relaxation channel in 2D is most probably associated with a fundamental difference in the electronic structures in 1D and 2D, viz., the occurrence of electronic energy states below the optical states in 2D, and their absence in 1D.

We are very grateful to T. Ogasawara and S. Uchida for their cooperation at the early stage of this work. We also thank M. Nagai and R. Shimano for stimulating discussions. This work was supported by a grant-in-aid for COE Research from the Ministry of Education, Science, Sports, and Culture of Japan and the New Energy and Industrial Technology Development Organization (NEDO). Work in Arizona was supported by the U.S. NSF.

REFERENCES

* Author to whom correspondence should be addressed. Electronic address:
gonokami@ap.t.u-tokyo.ac.jp

- [1] Y. Tokura *et al.*, Phys Rev. B **41**, R11657 (1990).
- [2] K. Matsuda *et al.*, Phys. Rev. B **50**, 4097 (1994); K. Matsuda *et al.*, Physica C **280**, 84 (1997).
- [3] R. A. Kaindl *et al.*, Science **287**, 470 (2000).
- [4] J. D. Perkins *et al.*, Phys. Rev. Lett. **71**, 1621 (1993).
- [5] J. Lorenzana and G.A. Sawatzky, Phys. Rev. Lett. **74**, 1867 (1995).
- [6] N. Motoyama, H. Eisaki, and S. Uchida, Phys. Rev. Lett. **76**, 3212 (1996).
- [7] H. Suzuura *et al.*, Phys. Rev. Lett. **76**, 2579 (1996).
- [8] M. Imada, A. Fujimori, and Y. Tokura, Rev. Mod. Phys. **70**, 1039 (1998).
- [9] T. Ogasawara *et al.*, Quantum Electronic and Laser Science Conference, Baltimore, 1999, p. 119; T. Ogasawara *et al.*, Phys. Rev. Lett. **85**, 2204 (2000).
- [10] H. Kishida *et al.*, Nature **405**, 929 (2000).
- [11] A. Schülzgen *et al.*, Phys. Rev. Lett. **86**, (2001) in press.
- [12] S.N. Dixit, D. Guo, and S. Mazumdar, Phys. Rev. B **43**, 6781 (1991).
- [13] D.S. Chemla and J. Zyss, *Nonlinear Optical Properties of Organic Molecules and Crystals*, (Academic, Orlando, 1987).
- [14] R.W. Boyd, *Nonlinear Optics*, (Academic Press, London, 1992).
- [15] Y. Mizuno *et al.*, Phys. Rev. B **62**, R4769 (2000).

FIGURES

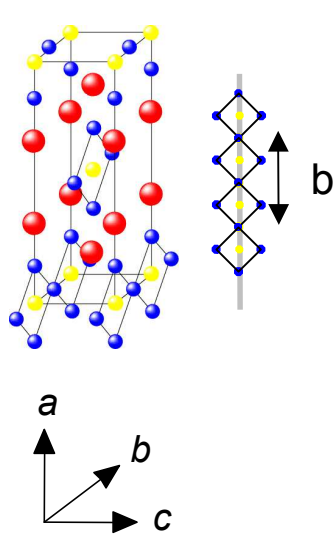
FIG. 1. Crystal structures of cuprates. (a) Sr_2CuO_3 ($b=3.91$ Å). (b) SrCuO_2 ($c=3.92$ Å). (c) $\text{Sr}_2\text{CuO}_2\text{Cl}_2$ ($a= b=3.98$ Å). Schematics of the Cu-O networks are also shown.

FIG. 2. Temporal profiles of $\Delta\alpha L$, which are normalized at their maximum values, at 290K in Sr_2CuO_3 (a), SrCuO_2 (b), and $\text{Sr}_2\text{CuO}_2\text{Cl}_2$ (c) for (pump + probe) energies of (1.46 + 0.95 eV) in the upper part and (0.95 + 1.03eV) in the lower part. One can observe that the picosecond decay components are pronounced for the higher pump photon energy. The upper panel shows $\Delta\alpha L$, now plotted on a logarithmic scale, for the upper cases ((a), blue; (b), green; (c), red) plotted against extended time scale. The black solid line shows a fitting curve to the $\Delta\alpha L$ of $\text{Sr}_2\text{CuO}_2\text{Cl}_2$ with two exponential functions with decay times of $\tau=1$ ps and $\tau=30$ ps.

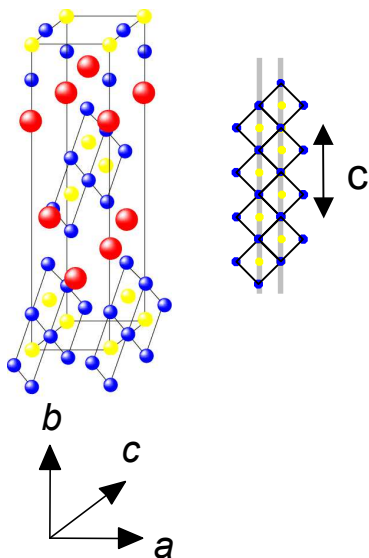
FIG. 3. TPA coefficient β versus $\omega_{pump} + \omega_{probe}$ at 290K in Sr_2CuO_3 (a), SrCuO_2 (b) and $\text{Sr}_2\text{CuO}_2\text{Cl}_2$ (c). Circles, squares and triangles correspond to pump energies at 1.46, 1.31 and 0.95 eV, respectively. Solid lines indicate the linear absorption α .

FIG. 4. Cluster models studied numerically and the corresponding energy levels in 1D (a) and 2D (b). Filled (open) circles are Cu (O) sites. Dashed lines denote mirror-plane symmetries used. States labeled * (1-photon states) have large dipole coupling to the ground state, those labeled # (2-photon states) have large dipole coupling to 1-photon states. See text for parameters.

(a) Sr_2CuO_3



(b) SrCuO_2



(c) $\text{Sr}_2\text{CuO}_2\text{Cl}_2$

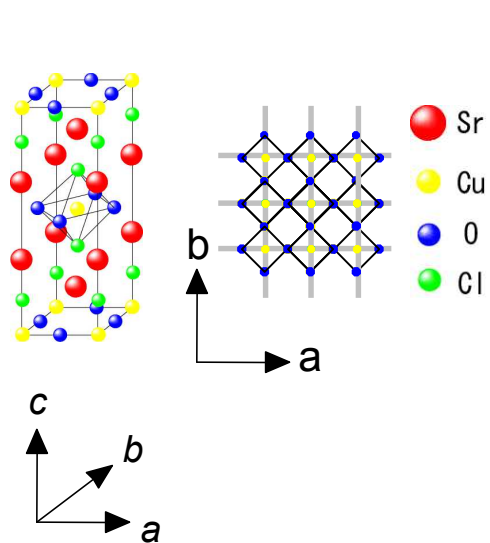


Fig. 1. M. Ashida *et al.*

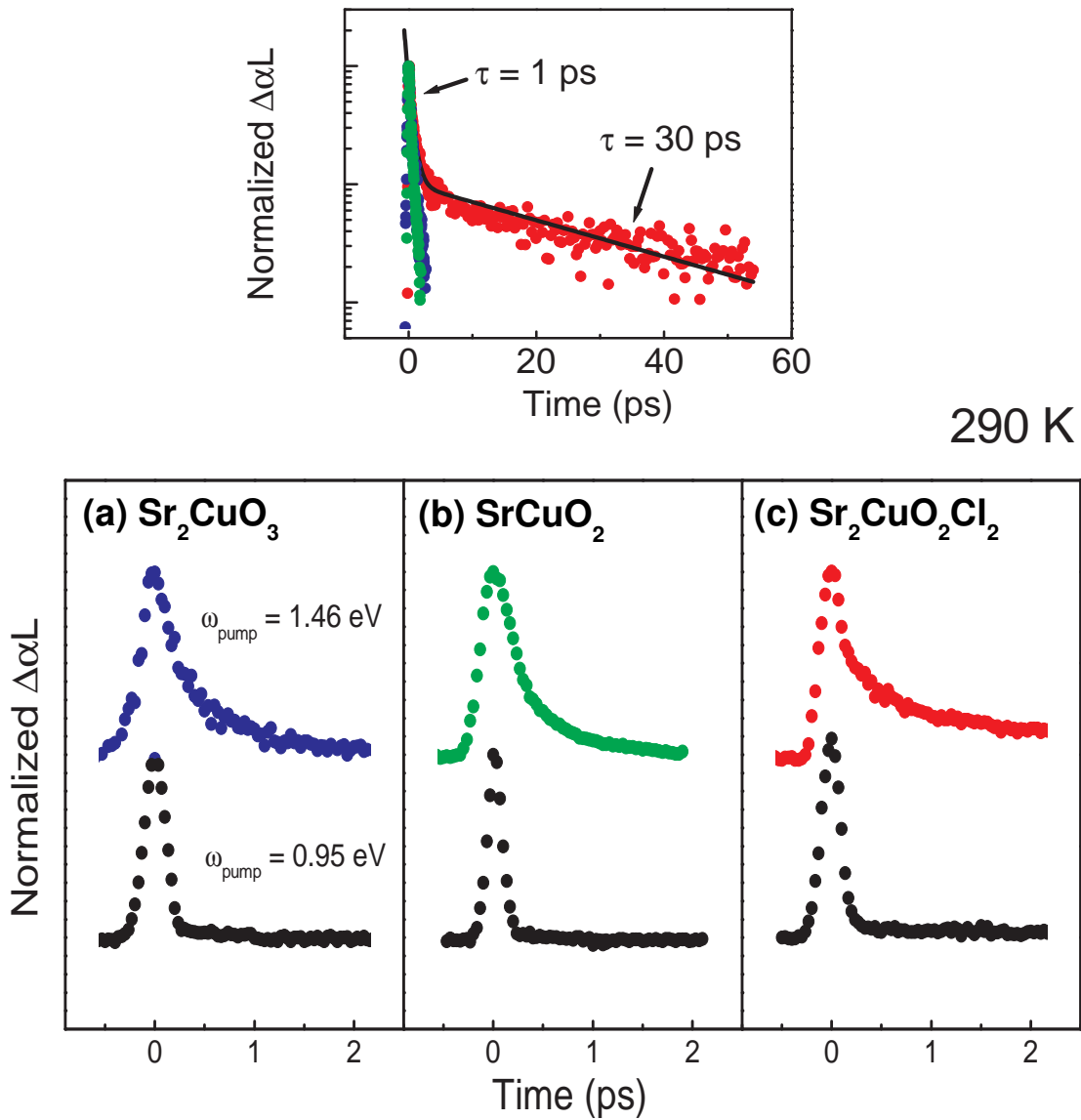


Fig. 2. M. Ashida *et al.*

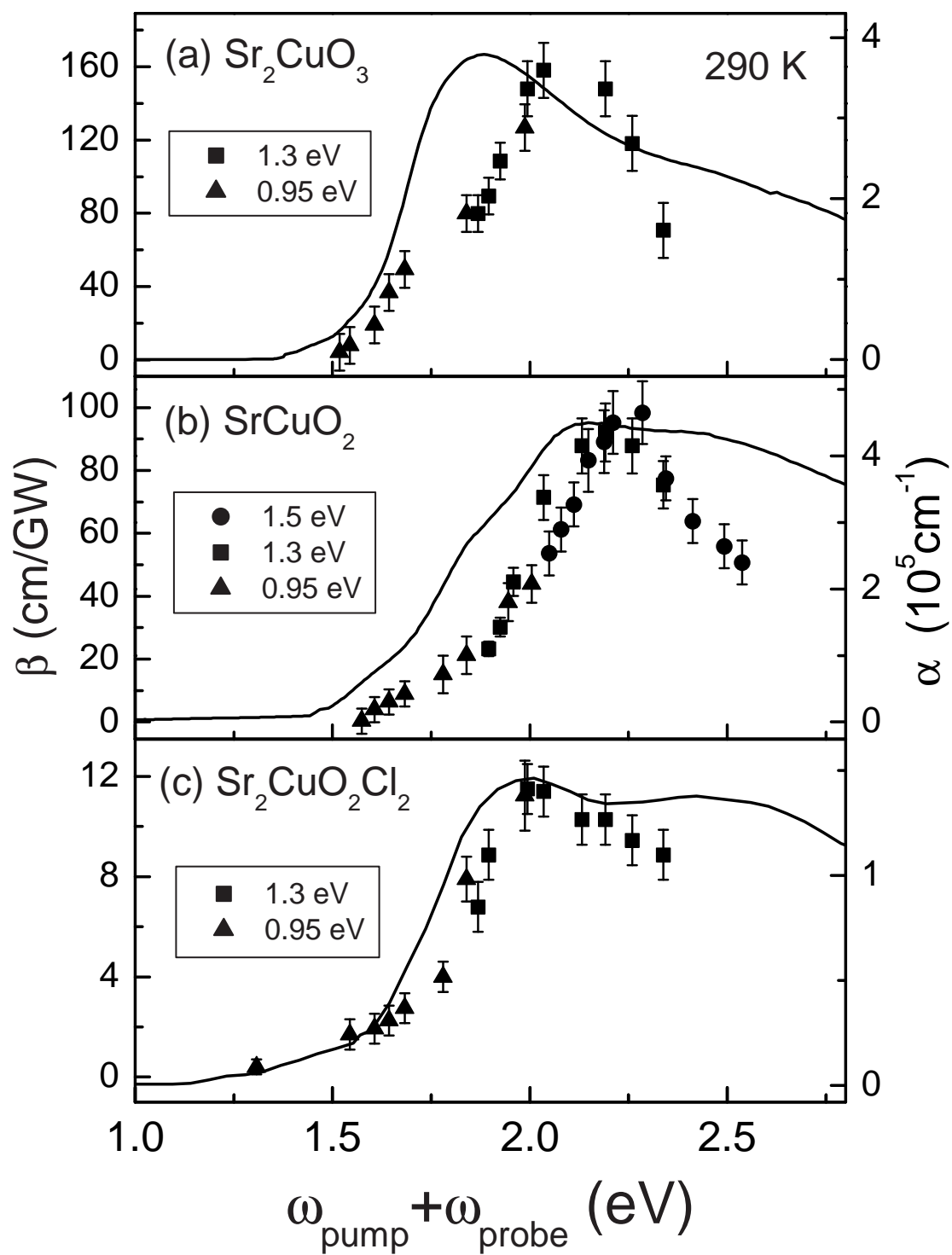


Fig. 3. M. Ashida *et al.*

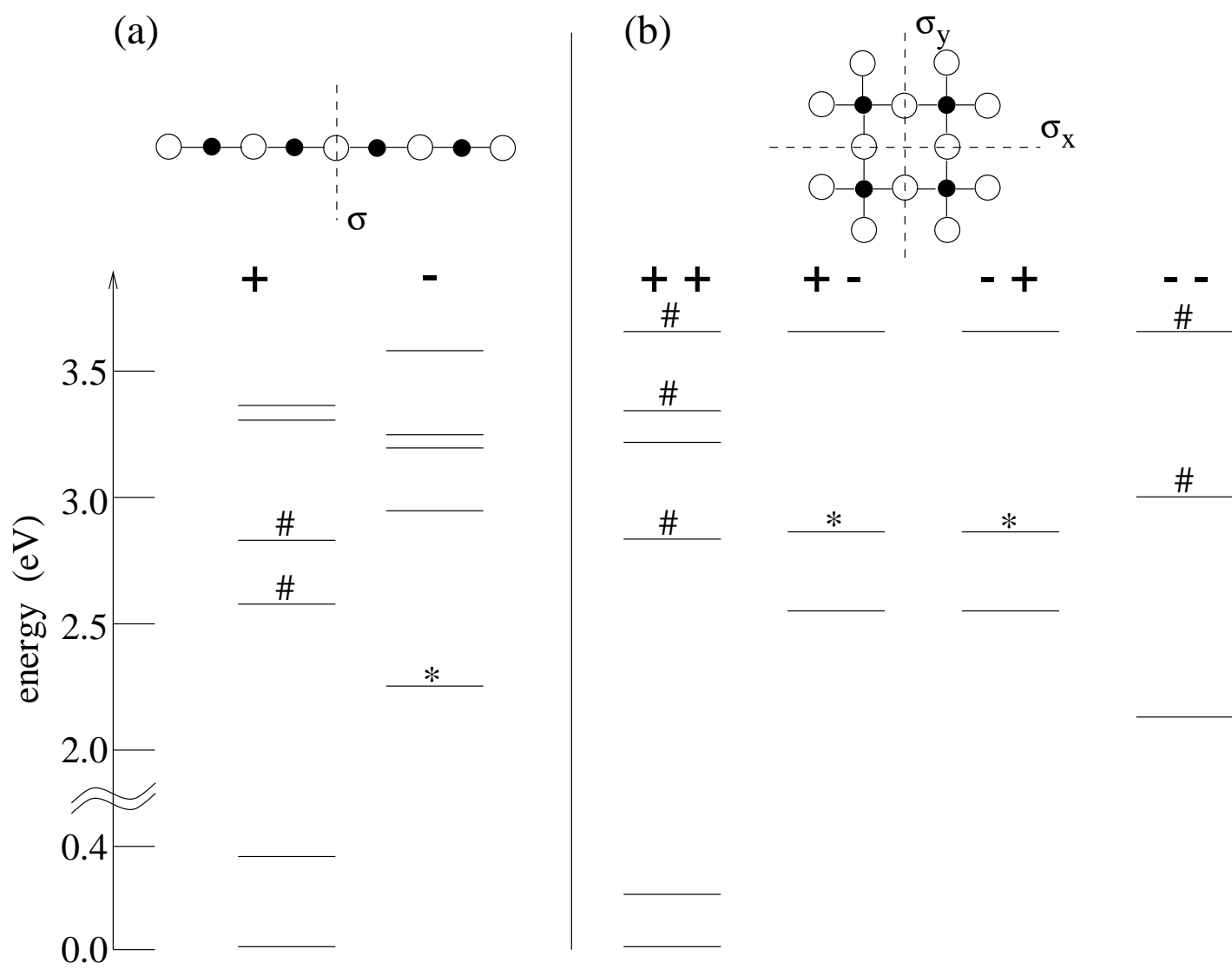


Fig. 4. M. Ashida et al.